



Numerical Simulation for Freeze Drying of Skimmed Milk with Moving Sublimation Front using Tri-Diagonal Matrix Algorithm

R. Naik, G. Arunsandeep and V. P. Chandramohan[†]

Department of Mechanical Engineering, National Institute of Technology Warangal, Warangal, Telangana-506 004, India

[†]Corresponding Author Email: vpcm80@nitw.ac.in

(Received August 11, 2016; accepted January 2, 2017)

ABSTRACT

Freeze drying is a highly advanced dehydration technique used for preserving pharmaceuticals, human organs transplanted to others and highly heat sensitive food products. During the freeze drying, there are two layers formed namely dried region and frozen region. In this present work, a numerical model is developed to estimate the temperature distribution of both regions. The sample object considered is skimmed milk. The transient heat conduction equations are solved for both regions of dried and frozen region. The interface layer between the two region is considered as moving sublimation front as same as the realistic case. Radiative boundary condition at the top and convective boundary condition at the bottom are considered. The model has been solved by finite difference method and the scheme used is backward difference in time and central difference in space (implicit scheme), which generates set of finite difference equations forming a Tri-Diagonal Matrix. A computer program is developed in MATLAB to solve the tri-diagonal matrix. The temperature distribution along the length of the product with varying chamber pressures and the sublimation front temperature with time are estimated. The transient effect of sublimation front movement was estimated with different applied chamber pressure. It was noticed that at lower pressure the sublimation rate is very fast.

Keywords: Freeze drying; Tri-diagonal matrix algorithm; Convective boundary condition; Radiative boundary condition; Implicit scheme; Sublimation front.

NOMENCLATURE

C_p	specific heat capacity	ρ	density
F	view factor for self-radiation flux	ϵ	vapour chamber emissivity
h_L	convective heat transfer coefficient	σ	Stefan-Boltzmann constant
ΔH_s	sublimation enthalpy		
k	heat conductivity	Subscripts:	
P_c	chamber pressure	l	dried layer
S	position of sublimation front	2	frozen layer
T	temperature	c	chamber
		i	initial
α	thermal diffusivity	L	shelf

1. INTRODUCTION

Freeze drying is a process of dehydration and it occurs below the triple point temperature of water. It is followed by freezing initially because of low temperature and then the product is experienced heavy vacuum pressure. Therefore, the product's frozen solid ice is directly sublimated to vapour phase without the formation of liquid phase. It has

wide varieties of applications such as drying of drug, pharmaceuticals, blood serum, human organs and highly perishable food materials. Though these applications are very expensive in nature, but their essentiality is very much important for the engineering stream.

There are few researches found in both experimental and numerical on freeze drying. A study on the freeze drying process by Milliman *et al.* (1985) used

a sorption-sublimation model. The shortest drying time was found when the pressure value was kept at its lowest value. At high temperature conditions sublimation is generally faster, but on overheating there is a loss of pore structure and it is called as a ‘collapse phenomenon’ (Pikal and Shah 2005) deteriorating the product quality. The sample temperature depends on the shelf temperature and the pressure applied in the chamber and could not be controlled directly during the drying process. In practice, trial-and-error experimental approach is used to find the suitable shelf temperature and chamber pressure empirically and therefore, many manufacturing process were not optimal. A report given by Toei *et al.* (1975) explaining the instability of the sublimation interface with a simple model. In this model the concept of zone sublimation was introduced. The stability criterion of sublimation plane was analyzed and it was found that the dependency is related to the physical properties of the porous bodies and on the drying conditions.

The glass transition temperature of food was the most important parameter which is responsible for the deterioration mechanism. The glass transition temperature also determines the stability of the food product. Glass transition temperature is experimentally determined for different products by variation of some thermodynamic or dielectric properties as a function of temperature (Roos 1992). A mathematical model was developed by Sadikoglu and Liapis (1997) to describe quantitatively the dynamic behavior of freeze drying stages of pharmaceuticals in trays. Classical mass and heat transfer equations were used to simulate the actual freeze drying processes in industry. The model calculations indicated that the contribution of the removal of bound water to total mass flux of the water which was removed during primary drying, was not significant. Therefore Sadikoglu and Liapis (1997) suggested that the mechanism of the removal of bound water could be neglected in the mathematical model during primary drying, without noticing any significant error in the theoretical results that were obtained from the solution of the model. Finite element analysis in two dimensional axisymmetric space has been considered by Mascarenhas *et al.* (1997). This model calculated the variation of partial pressure of water vapour, the temperature and the concentration of sorbed water. Lagrangian-Eulerian method was used to model the sublimation front of freeze drying process which is the surface which separates the frozen and dried region. The developed finite element practice provided valuable information on primary and secondary drying stages.

Hammami and Rene (1997) worked on the production of high-quality freeze dried strawberry pieces by the response surface method. It was a quadratic model. Trial experiments were conducted to obtain the fitting surfaces and this model was used to predict the optimal solution. A software tool was developed for interactive selection of operating condition for freeze drying process in order to maximize the efficiency in terms of productivity and product quality and it was found that the product temperature was the most

determinant one (Trelea *et al.* 2007).

There were not much detailed study on freeze drying on both experimentally and numerically as both ways have their own practical complexity. From the literature it is found that the complexity of the numerical solution is high as it has two regions (dried and frozen regions) and both the regions were separated by a moving sublimation front. It is necessary to estimate the product temperature during drying at different chamber pressure as it allows the maintenance of product quality and also to reduce the process cycle time. It is also used for process industries to optimize their insulation thickness, to design their instruments etc. Modelling makes it easy to understand the process, the variation on cycle time, product temperature, the effect of pressure and other parameters, thereby, facilitate process of further research and development.

Hence the main objectives of the present work are mentioned as follows: (i) To develop a numerical model for freeze drying through discretization of governing equations and the boundary conditions using implicit scheme in finite difference method, (ii) To incorporate the convective and radiative boundary conditions for heating the product during freeze drying, (iii) To develop a MATLAB program to study the effect of the pressure and temperature on the freeze drying process and analyze the sublimation front temperature after optimizing the number of grids and time steps through grid and time independency test, (iv) To study the temperature variation within the product in the frozen and dried region with time at different applied pressure and (v) To study the nature of progress of sublimation front in different temperature and pressure conditions.

2. METHODOLOGY

2.1 Material and Geometry

The material selected for the analysis is skimmed milk and the geometry of the sample is taken as a slab of thickness 10 mm and it is shown in Fig 1.

The properties of skimmed milk are mentioned in Table 1. The top surface is assumed as $x = 0$, the downward direction as the positive direction for analysis and the bottom surface is taken as $x = L$.

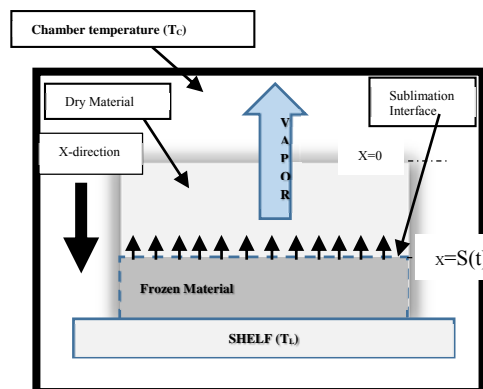


Fig. 1. Scheme of freeze drying sublimation interface

Table 1 Properties of frozen and dried region of skimmed milk

Symbol	Property	Value in SI units
ρ_1	dried layer density	445 kg/m ³ (Mascarenhas <i>et al.</i> 1997)
ρ_2	frozen layer density	1058 kg/m ³ (Mascarenhas <i>et al.</i> 1997)
C_{p_1}	Specific heat capacity of dried layer	2595 J/kgK (Mascarenhas <i>et al.</i> 1997)
C_{p_2}	Specific heat capacity of frozen layer	1967.8 J/kgK (Mascarenhas <i>et al.</i> 1997)
k_1	dried layer heat conductivity	2.706×10^{-2} W/m K (Mascarenhas <i>et al.</i> 1997)
k_2	frozen layer heat conductivity	2.4 W/m K (Mascarenhas <i>et al.</i> 1997)
ϵ	vapor chamber emissivity	0.94 (Pikal and Shah 1990).
F	view factor for self-radiation flux	0.99 (Pikal and Shah 1990).
ΔH_s	sublimation enthalpy	2.79×10^6 J/kg (Mascarenhas <i>et al.</i> 1997)
σ	Stefan-Boltzmann constant	5.6704×10^{-8} W/m ² K ⁴
T_i	Initial Temperature	227 K
T_c	chamber temperature	198 K
T_L	Shelf temperature	263 K
P_c	chamber pressure	10 - 40 Pa
α_1	dried layer thermal diffusivity	2.3433×10^{-08} m ² /s
α_2	frozen layer thermal diffusivity	1.1528×10^{-06} m ² /s
h_L	convective heat transfer coefficient	1.5358 P _c W/m ² K (Sadikoglu and Liapis 1997)

The physical parameters of skimmed milk are taken from literatures (Millman *et al.* 1985; Sadikoglu and Liapis 1997; Mascarenhas *et al.* 1997). In the industries, the milk product was initially frozen by a deep freezer and then into the freeze dryer where the condenser temperature was maintained at -80 °C (Roos 1992). Therefore, a reasonable assumption is made in this work that the initial temperature of milk is 227 K (-46 °C). The chamber is evacuated and the chamber pressure is reduced to a very low value so that sublimation takes place. When sublimation starts from the top of the product wall (at $x = 0$) simultaneously the heat is supplied to the product from the bottom wall ($x = 10$ mm). In order to have further sublimation from the product, the latent heat of sublimation must be supplied from a heat source. For further encouraging the sublimation, the chamber temperature is increased which results in radiation heat supplied to the product. Thus, the boundary conditions are considered as radiative in nature from the top surface and convective from the bottom surface. For the heat transfer analysis, the product is assumed to be as a slab and transient heat transfer by one dimensional approach. The sublimation is assumed to be occurring uniformly giving rise to a uniform interface known as sublimation interface or sublimation front and hence the sublimation front is moving with respect to time when the drying progresses. At the starting of the analysis, it is considered as 2% of the total length is in the dried region, therefore, the interface position or the sublimation front lying at 0.2 mm.

2.2 Assumptions

The following assumptions are to be considered:

(i) One dimensional transient heat transfer is considered, (ii) The frozen and dried regions have uniform heat and mass transfer properties throughout the region, (iii) There is a sublimation front which is a continuous interface lying between the dried and the frozen region with negligible thickness, (iv) Dimensional changes in the material are negligible and (v) The porous matrix structure is rigid and permeable and circulation of vapour fluxes are allowed.

2.3 Governing Equations

The governing equation for heat transfer analysis is 1D transient conduction equation which is second order partial differential nature.

$$\frac{\partial T_1}{\partial t}(x, t) = \alpha_1 \frac{\partial^2 T_1}{\partial x^2}(x, t), \forall x \in (0, S(t)) \quad (1)$$

$$\frac{\partial T_2}{\partial t}(x, t) = \alpha_2 \frac{\partial^2 T_2}{\partial x^2}(x, t), \forall x \in (S(t), L) \quad (2)$$

Where, T_1 and T_2 are temperatures in dried region and frozen region in K respectively, α_1 and α_2 are the thermal diffusivities of dried and frozen region in m²/s respectively, x is the direction of the moving sublimation front and t is the time elapsed during the analysis in s.

Eq. (1) is valid for the dried region which ranges from the top of the sample i.e. from $x = 0$ to $x = S(t)$ and Eq. (2) is valid for the frozen region which ranges from $S(t)$ to L . Here $S(t)$ is the position of the sublimation front with respect to time which moves downward.

2.4 Boundary and Initial Condition Conditions

From the top surface of the product ($x = 0$), the main heat transfer mode is through radiation and from the

bottom surface ($x = L$), it is convection heat transfer mode.

This gives two Neumann-type boundary conditions:

$$-k_1 \frac{\partial T_1}{\partial x}(x, t) = \sigma \in F (T_c^4 - T_1^4), \quad x = 0 \quad (3)$$

$$-k_2 \frac{\partial T_2}{\partial x}(x, t) = h_L(T_L - T_2), \quad x = L \quad (4)$$

Where, T_L is shelf temperature in K, T_C is chamber temperature in K, k_1 and k_2 are the thermal heat conductivities of dried and frozen region in W/m K respectively, σ is the Stefan-Boltzmann constant, 5.6704×10^{-8} W/m² K⁴, \in is the vapour chamber emissivity, F is view factor for self-radiation flux, h_L is convective heat transfer coefficient in W/m²K depending on the chamber pressure. The relationship is given by Sadikoglu and Liapis (1997)

$$h_L = 1.5358 P_c \quad (5)$$

For solving the Eqs. (3 and 4), continuity of temperature across the sublimation front should be imposed:

$$T_1 = T_2 = T_s, \quad x = S(t) \quad (6)$$

The sublimation front is a moving with respect to time. It is an evolving boundary between the two phases and the phase boundary is moving with time. It gives an extra boundary condition called the Stefan condition (Crank 1984) at $x = S(t)$,

$$k_2 \frac{\partial T_2}{\partial x}(x, t) - k_1 \frac{\partial T_1}{\partial x}(x, t) = \Delta H_s(\rho_2 - \rho_1) \frac{\partial S(t)}{\partial t} \quad (7)$$

Here, the net heat supplied to the interface is in the left hand side of Eq. (7) and it is used for the sublimation of ice into vapour and therefore it is equated to the right hand side of Eq. (7) which is the sublimation term.

The initial condition is at $t = 0$ s, $T = T_i$

2.5 Discretization

All the transient governing equations and boundary conditions are discretised using finite difference method and an implicit scheme. Backward difference in time and central difference in space are considered. This gives a set of equations which form a tri-diagonal matrix.

A computer code in MATLAB is developed to solve this tri-diagonal matrix through the tri-diagonal matrix algorithm (TDMA). Temperature distribution throughout the product at different chamber pressure is estimated.

3. RESULTS AND DISCUSSIONS

3.1 Grid and Time Independency Test

A time independent test (Fig. 2a) is performed with different time steps dt (5, 10, 20, 50, 75 and 100 s). As it is seen that the difference between the time steps 100, 75, 50 and 20 s are comparable, but there is not much variation noticed between the time steps of 5 and 10 s.

Hence the remaining simulations are carried out with the time step of 10 s. Grid independent test was

conducted by varying grid step dx and it is shown in Fig. 2(b). The error percentage is sufficiently small for 120 and 140 nodes. Therefore, the number of nodes selected for this analysis is 120.

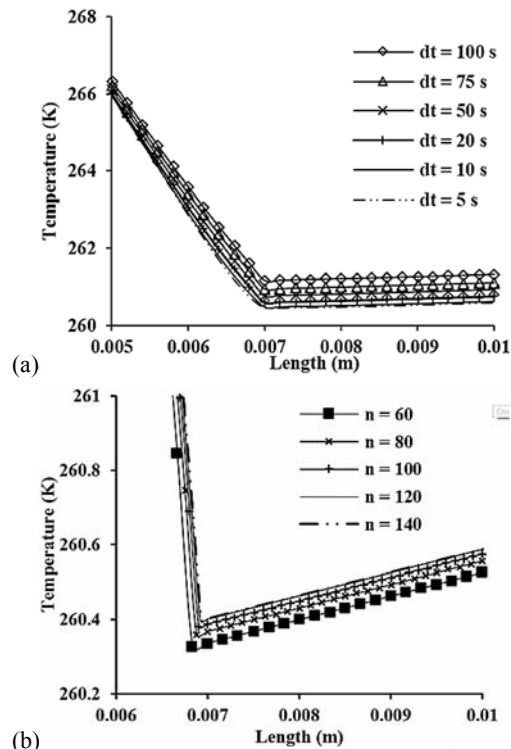


Fig. 2. (a) Time independency test ($P_c = 40$ Pa) and (b) Grid independency test ($P_c = 40$ Pa and $dt = 10$ s).

3.2 Temperature Distribution of Skimmed Milk at Different Chamber Pressure

The transient temperature profiles of skimmed milk at different chamber pressures (10, 20, 30 and 40 Pa) are plotted and are shown in Figs. 3a to d. The initial temperature distribution at $t = 0$, which is almost similar for all the chamber pressure considered in this work. Fig. 3a is drawn at chamber pressure at 10 Pa. At $t = 1$ hr, the temperature decreases from the top surface of the sample (at $x = 0$) from 247.24 to 234.55 K (at $x = 1.58$ mm). This region is called dried region. The thermal conductivity of the dried region is low therefore, the temperature is decreased during this dried region. The second region (from $x = 1.58$ to 10 mm) is called frozen region and here, the temperature increases to 235.95 K at $x = 10$ mm (bottom surface). The other time considered here ($t = 2, 5$ and 10 hr) also has similar type temperature profile and have two regions. These 2 regions have different thermal properties, therefore, the nature of curve also different.

Similar analysis is performed for higher pressure, 20, 30 and 40 Pa (Fig. 3b, c and d), similar nature of curves are seen but at an elevated temperature. The temperature is increased significantly (when the chamber pressure increased from 10 to 40 Pa) in the first hour of analysis itself.

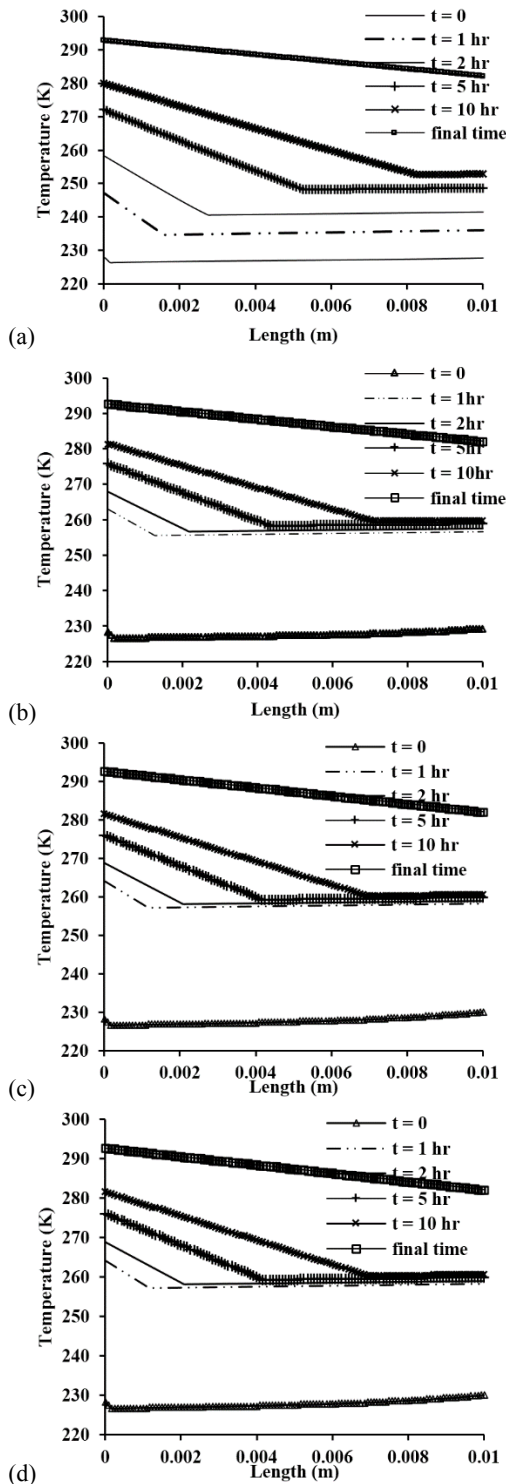


Fig. 3. Temperature distribution of skimmed milk at different chamber pressures, (a) $P_c = 10$, (b) 20, (c) 30 and (d) 40 Pa.

3.3 Effect of Pressure on Temperature Profile

The temperature profile within the sample is analyzed at $t = 10$ hr as shown in Fig. 4. The temperature at the top surface ($x = 0$) has reached almost same values (varied from 279.97 to 281.66 K) for different pressure ranged from 10 to 40 Pa. The temperature at bottom surface (at $x = 10$ mm) are varied as 252.8, 258.03,

259.83 and 260.58 K for different chamber pressure at 10, 20, 30 and 40 Pa respectively. This suggests that after 10 hr of drying, the temperature of the dried region are less dependent on the chamber pressure hence there is less variation whereas the frozen region temperatures are more dependent on pressure thereby leaving a significant difference. Also, the convective heat transfer coefficient is a function on chamber pressure and hence the rate of heat transfer from the bottom plate at $x = 10$ mm is dependent on the chamber pressure.

It is also seen from Fig. 4 that the temperature variation is very small for 30 and 40 Pa, whereas there is significant variation at lower chamber pressure as seen for 20 and 10 Pa. This nature of the temperature is due to the sublimation which is occurring at a faster rate at lower chamber pressure.

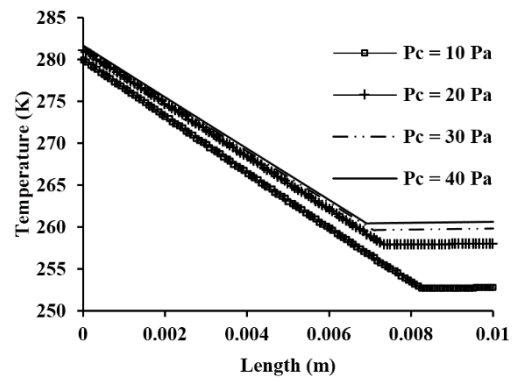


Fig. 4. Temperature Profile with different pressure at $t = 10$ hr of operating time.

3.4 Effect of pressure on temperature profile

The variation of sublimation front temperature with time for different pressure is shown in Fig. 5. At all the pressure considered in this work (10 to 40 Pa), the sublimation front temperature is increased when time increases. At 10 Pa the sublimation front temperature rises gradually from 227 K (initial temperature) to 252.63 K. Whereas at 40 Pa, the temperature very rapidly increases from 227 to 257 K in the first 1800 s and then it rises very slowly and reaches to 260.4 K in 10 hr.

From Fig. 5 it is also noticed that at high pressure, the sublimation front temperature suddenly rises in the initial span of total time whereas at low pressure the sublimation front temperature rises gradually. This happens because at high pressure the sublimation rate is slow. The heat is dissipated in the sample and the temperature of the sample increases at a faster rate, whereas at low pressure, the sublimation occurs at a faster rate. For the same amount of heat supplied, at low pressure, most of the heat is taken by the latent heat of sublimation and the temperature rise of the sample is not so significant. The sublimation front temperature has a very small rise at the later stage (for example at $p = 40$ Pa, the temperature more than 1800 s) of the analysis. Once the sublimation front temperature approaches the plate temperature, there is no further significant rise in temperature and the curves become flatter at the later stage.

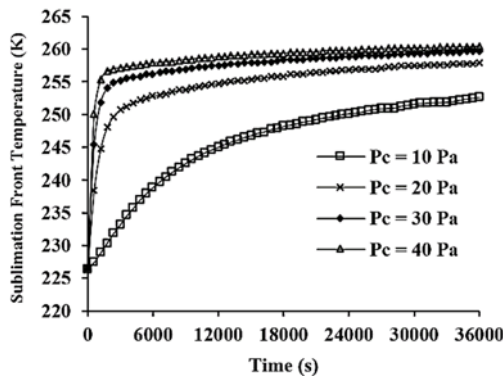


Fig. 5. Variation of Sublimation front temperature with time for different pressures.

3.5 Sublimation Front Position with Time for Different Pressures

The progress of sublimation front position with respect to time for different pressure is mentioned in Fig. 6. The slope of a position vs time plot gives the instantaneous velocity and hence in this Fig. 6 the instantaneous velocity of the sublimation front can be compared at different chamber pressure. After 10 hr of drying, it is noticed that the sublimation front reaches 8.27 mm at 10 Pa, 7.39 mm at 20 Pa and 7.1 mm at 30 Pa and 6.96 mm at 40 Pa. Thus the sublimation front progresses at a faster rate at low pressure and slower rate at high pressure. This suggests that the sublimation is occurring at a faster rate at low chamber pressure. Also it is observed that the drying time required for the low chamber pressure is less than the drying time required at a high chamber pressure.

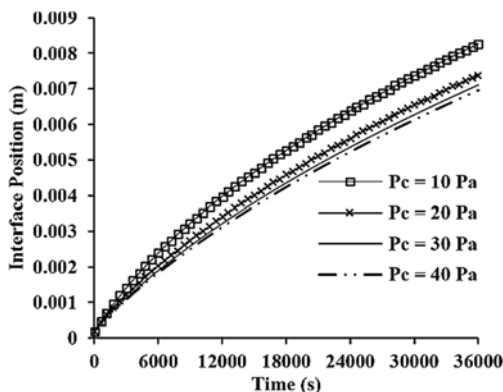


Fig. 6. Sublimation front position with time at different chamber pressure.

4. CONCLUSION

A finite difference approach was used to model the freeze drying of skimmed milk. 1D domain has been selected for this approach. A computer code was developed in MATLAB to solve the governing equations. Temperature profile of dried region and frozen region were estimated at different chamber pressure. Temperature of the dried region decreased towards down from top as this region's conductivity is low. Similarly, a slight rise in temperature in the frozen

region was noticed because of its higher thermal conductivity than dried region. After 10 hr of drying, chamber pressure did not make much impact on the temperature of the dried region. At the same time, it gave much impact on frozen region, therefore huge temperature difference was noticed. At lower pressure the sublimation front temperature increased gradually and at higher pressure it increased in very steep manner and later it did not give much variation. The product's sublimation front reached at 8.27, 7.39, 7.1 and 6.96 mm at different chamber pressure 10, 20, 30 and 40 Pa respectively after 10 hr of drying. Thus it is proved that at lower pressure the sublimation front moved quickly. Therefore, it is concluded that the developed model is able to predict the transient temperature profiles at different chamber pressures and the nature of sublimation front movement with respect to time and distance.

REFERENCES

- Crank J. (1984). *Free and Moving boundary Problems*. Clarendon Press, Oxford, UK.
- Hammami, C. and F. René (1997). Determination of freeze drying process variables for strawberries. *Journal of Food Engineering* 32(2), 133–154.
- Mascarenhas, W. J., H. U. Akay and M. J. Pikal (1997). A computational model for finite element analysis of the freeze drying process. *Computer Methods on Applied Mechanics and Engineering* 148, 105–124.
- Millman, M. J., A. I. Liapis and J. M. Marchello (1985). An analysis of the lyophilisation process using a sorption–sublimation model and various operational policies. *AICHE Journal* 131(10), 1594–1604.
- Pikal, M. J. and S. Shah (1990). The collapse temperature in freeze drying: dependence on measurement methodology and rate of water removal from the glassy state. *International Journal of Pharmacy* 62, 165–186.
- Roos, Y. (1992). Phase transitions and transformations in food systems. In D. R. Heldman, and D. B. Lund, (Eds.), *Handbook of food engineering*. New York: Marcel Dekker.
- Sadikoglu, H. and A. I. Liapis (1997). Mathematical modelling of the primary and secondary drying stages of bulk solution freeze drying in trays: parameter estimation and model discrimination by comparison of theoretical results with experimental data. *Drying Technology* 15 (3-4), 791–810.
- Toei, R., M. Okazaki and M. Asaeda (1975). The stability of plane sublimation and a model of zone sublimation in freeze drying of porous bodies. *Journal of Chemical Engineering of Japan* 8(4), 282–288.
- Trelea, I. C., S. Passot, F. Fonseca and M. Michele (2007). An interactive tool for the optimization of freeze drying cycles based on quality criteria. *Drying Technology* 25, 741–751.

